AIAA 80-0441R

Adaptive-Wall Wind-Tunnel Development for Transonic Testing

Bodapati Satyanarayana*
Joint Institute for Aeronautics and Acoustics, Stanford University, Stanford, Calif.
and
Edward Schairer† and Sanford Davis‡
NASA Ames Research Center, Moffett Field, Calif.

In principle, the adaptive-wall wind tunnel is an attractive alternative to traditional methods of accounting for wind-tunnel wall interference. The concept has been successfully demonstrated for two-dimensional flows at moderately supercritical Mach numbers, but more work needs to be done before the method can be used in production testing. In this paper experimental techniques for rapid assessment and correction of wall interference are described. The procedure is based on laser velocimetry measurements on two control surfaces and on the use of a dedicated computer for rapid data processing. The experimental arrangement and instrumentation are described and typical results from an experiment on a nonlifting NACA 0012 airfoil at $M = 0.78$ are discussed.

Nomenclature

c = airfoil chord
C_p = pressure coefficient: $(p - p_\infty) / [(\frac{1}{2})\rho V_\infty^2]$
M = Mach number, subscript
p = static pressure
u = axial perturbation velocity component
v = normal perturbation velocity component
x = axial distance
y = distance normal to x axis
α = angle of attack
ρ = density

Subscripts

$c1$ = calculated value at level 1
$c2$ = calculated value at level 2
$m1$ = measured value at level 1
$m2$ = measured value at level 2
∞ = freestream
$1, 2$ = at levels 1 and 2

I. Introduction

An adaptive-wall wind tunnel is a wind tunnel in which wall interference is either eliminated or reduced to a minimum by actively controlling the boundary conditions at the walls of the tunnel. In addition to the obvious benefit of eliminating the need to correct wind-tunnel data for wall interference, an adaptive-wall wind tunnel would allow larger models to be tested at higher Mach numbers and higher angles of incidence than would be possible in a conventional wind tunnel of the same size. This is a potentially attractive alternative to the elimination of wall interference by attempting to account for interference analytically.

Wall interference, which is a particularly serious problem in transonic wind tunnels, depends on a large number of flow parameters, including Mach number, model size, model incidence, and blockage ratio. Tunnel characteristics, such as the type of wall ventilation (slotted or perforated), the percentage of ventilation, and the distribution of ventilation are also important.

Wall geometries of conventional transonic test sections are designed to minimize wall interference during transonic testing over a range of test parameters. Wall corrections based on the classical linear theory provide simple formulas that can be easily implemented. However, the theory is not adequate for the transonic regime where nonlinear effects are important. The adequacy of the homogeneous wall boundary condition also is questionable. Generally, wall corrections for a particular facility are determined based on the test results of calibration models of different blockage and chord-to-height ratio. In such cases, nonlinear effects are included but the results of calibration models may not be universally applicable for other models. For general testing purposes, model blockage ratios are usually limited to a conservative value of about 1%.

Kemp,[1,2] Stahara,[3] and Murman[4] developed methods to assess the wall interference using measured pressures near the tunnel wall and on the model. Nonlinear transonic theories are employed in these assessments. Although there is a certain amount of uncertainty, and their utility is limited to attached flows, these methods with further improvements may be of value for assessing the wall interference until present-day passive wall tunnels are phased out in favor of active wall tunnels or in cases where residual wall interference is small enough to be adequately predicted by these methods.

The idea of an accommodating wall to reduce wind-tunnel interference is not new. The concept was investigated in Britain over 30 years ago, but without much success.[5] Recently, the idea was expanded to the adaptive-wall concept by Ferri and Baronti[6] and by Sears.[7] Some recent contributions to the theory of adaptive walls are given in Refs. 8-10.

Using the adaptive-wall method, it is possible to obtain interference-free flow for a given Mach number and model configuration; however, the required wall boundary conditions are different for each flow condition. Variable wall boundary conditions can be achieved by the following methods: 1) local plenum pressure control (ventilated walls), 2) localized wall contour control (streamlined solid walls), 3) local cross-flow characteristic control (variation of porosity and hole angle), and 4) a combination of 1 and 3.

The feasibility of the first method was evaluated at Calspan[11,12] by theoretical and experimental methods. The feasibility of the second method is being developed at Southampton[13] and in Berlin.[14] The method of local crossflow control by variation of hole angle is being explored

Submitted March 17, 1980; presented as Paper 80-0441 at the AIAA 11th Aerodynamic Testing Conference, Colorado Springs, Colo., March 18-20, 1980; revision received Aug. 26, 1980. This paper is declared a work of the U.S. Government and therefore is in the public domain.

*Engineering Senior Research Associate, Department of Aeronautics and Astronautics. Member AIAA.
†Research Scientist.
‡Research Scientist. Associate Fellow AIAA.

at AEDC.[15] Most of the work on adaptive walls is still in the technology-development phase; however, the concept has been shown to be feasible, and it is likely that production facilities will be built before long.

The present paper describes a new adaptive-wall wind tunnel designed for two-dimensional testing. The tunnel advances the state of the art in three areas: 1) the use of laser velocimetry for the assessment of wall interference, 2) computer-experiment integration for real-time data acquisition and on-line interference assessment, and 3) use of a measured influence coefficient matrix for rapid convergence to an interference-free flow.

The approach used at Ames Research Center is based on the method of local plenum control, but with a slotted rather than a perforated wall geometry. The purpose of this paper is to describe the method whereby the new elements just enumerated were incorporated into an efficient scheme for rapid convergence to an interference-free transonic flow. In this preliminary study only linearized theory was used for interference assessment at the control surface, but the experimental results will show that even a well-developed transonic flow can be controlled with the present adaptation.

II. Adaptive-Wall Concept

Ferri and Baronti[6] and Sears[7] arrived at the adaptive-wall concept by recognizing that local wall properties can be systematically varied to achieve unconfined flow by measuring two flow quantities and evaluating the requisite functional relationship for unconfined flow. These investigators used the perturbation quantities u and v at one control surface to establish the unconfined flow. In the experimental implementation, static pressure and flow angle were measured to evaluate u and v. In the present investigation, however, vertical velocity perturbations at two levels (Fig. 1) were used to establish the unconfined flow. Because only one component of the velocity has to be measured, this method simplifies the experimental technique. In the present tests, measurements were made with a laser velocimeter.

Unconfined flow conditions can be produced in the test section by systematically adjusting the local wall characteristics until the measured vertical velocity distribution at a control level corresponds to that which would exist in free air. The iterative procedure used to converge on the interference free flow is illustrated schematically in Fig. 2. After the desired upstream tunnel conditions are established, the vertical velocity distributions (v_{m1} and v_{m2}) are measured at two levels, as shown in Fig. 2. Using the measured vertical velocity distribution at level 1 as a boundary condition, the interference-free vertical velocity distribution at level 2, v_{c2}, is calculated using linear compressible theory and unconfined-flow boundary conditions at infinity. If the measured velocities at level 2, v_{m2}, and the calculated values v_{c2} do not agree, then the flow is not interference-free and wall adjustment is necessary. The pressures in plenum compartments above and below the test section are changed in accordance with measured relationships between plena pressures and vertical velocities at level 2 (influence coefficients). The entire process is then repeated until the differences between the measured and computed velocity distributions at level 2 are within experimental error. At this point wall interference has been eliminated and the free-air model pressure distribution is measured.

In this paper a sample case showing convergence to interference-free flow is presented. A detailed description of the calculations and more complete experimental results will be presented in a subsequent paper.

III. Experimental Apparatus

A. Test Section

The 25 × 35-cm low-speed in-draft tunnel at Ames Research Center was modified to one with a 25 × 13 cm transonic test section (Fig. 3). New upper and lower surfaces are formed by walls with 10 slots that have an open area ratio of 12%. The walls are diverged 0.1 deg to compensate for boundary-layer growth. Upper and lower plenum chambers have a depth of 11 cm and are divided into 20 compartments (10 above and 10 below) by transverse inserts. The spacing, and thus the number of compartments, can be varied in steps of 2.54 cm. The configuration for the tests reported here is shown in Fig. 4. The minimum spacing of 2.54 cm is provided in the model region where the largest gradients are expected.

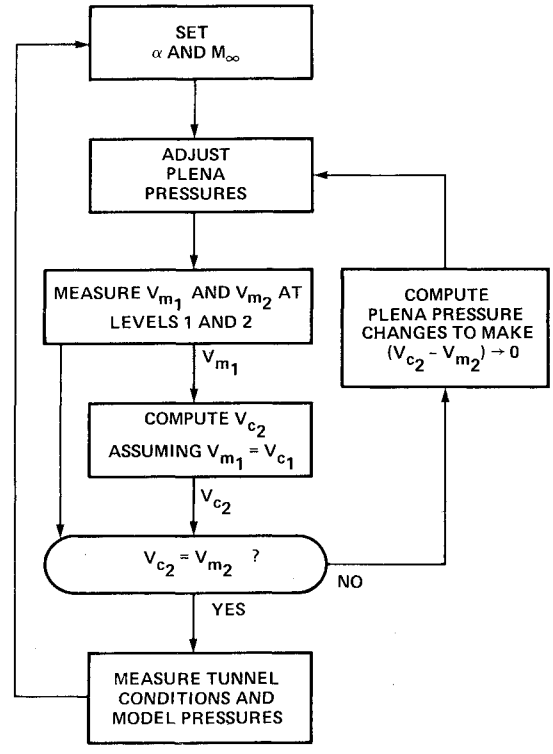

Fig. 2 Adaptive-wall wind-tunnel scheme.

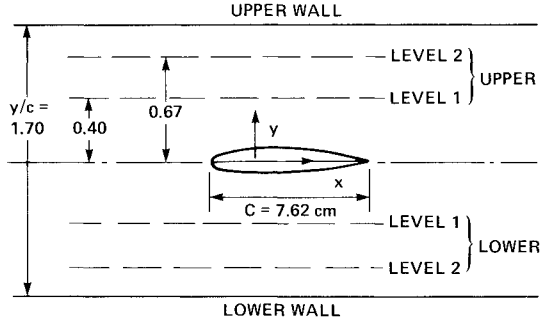

Fig. 1 Vertical velocity control surface locations.

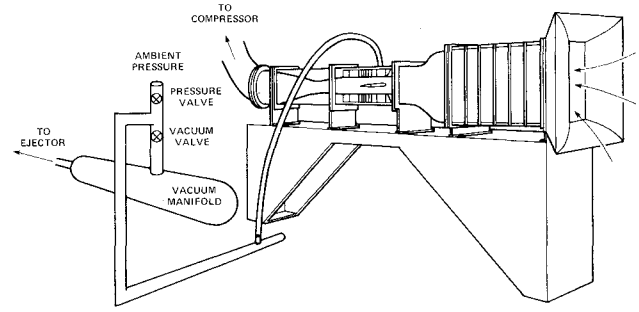

Fig. 3 25 × 13 cm adaptive-wall transonic tunnel.

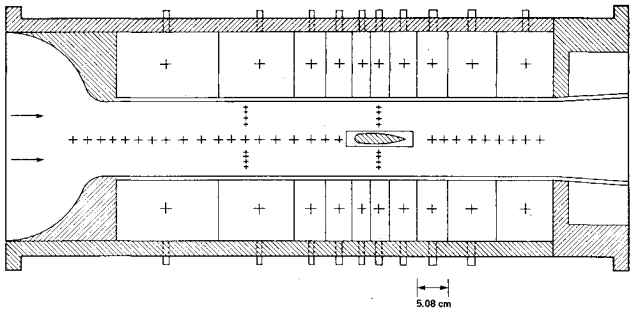

Fig. 4 25 × 13 cm adaptive-wall test section.

Each compartment is connected to an auxiliary air system, either to add or remove air as required. Since the facility is an atmospheric stagnation pressure tunnel, mass addition is accomplished by opening a valve to the atmosphere. An air ejector was used as the vacuum source to remove the appropriate quantity of mass from each plenum compartment. The ejector is connected to a vacuum manifold to which all 20 plenum compartments are connected. Figure 3 illustrates how a typical plenum compartment is connected to the auxiliary air system. Identical tubing and valves connect all other compartments in a similar manner. The auxiliary air system was designed to add or remove up to 10% of the test-section mass flow.

The test-section Mach number is controlled by a downstream flexible converging-diverging throat section. The tunnel is usually operated with a choked throat to minimize noise propagating upstream from the control valve and to obtain a steady Mach number in the test section. The downstream portion of the tunnel is connected to a vacuum sphere by a gated control valve.

B. Model

The NACA 0012 airfoil section was selected for testing because abundant data are available from various sources for comparison. A model with a 7.62 cm (3 in.) chord and 25 cm (10 in.) span was instrumented with 16 static pressure orifices on the upper surface and 9 on the lower surface (Fig. 5). The experiments were conducted with and without a boundary-layer trip. The trip was formed by randomly applied glass beads, 0.127 mm (0.005 in.) in diameter, on the upper and lower surfaces, beginning at 10% chord and extending over a width of 2.54 mm.

IV. Instrumentation

The adaptive-wall wind-tunnel instrumentation includes conventional pressure instruments for measuring the test section Mach number distribution, plenum pressures, and model pressure distribution, and a laser velocimeter for measuring vertical velocity components in the test section.

A. Pressure Instrumentation

All test section and model pressures were measured using a four-unit Scanivalve pressure transducer coupled to a minicomputer. In addition, ambient pressure, temperature, and calibration pressure were simultaneously recorded. The Scanivalve transducer calibration constants were obtained routinely every time the Scanivalve was operated. Test-section and plenum pressures were also displayed on a manometer board.

B. Laser Velocimetry

Several methods were available for measuring flowfield disturbance velocities. Conventional probes, such as pitch probes, hot films, and hot wires could be used; however, they interfere with the flow, and the magnitude of the interference has to be carefully studied. Probe interference is especially important because small perturbation quantities were to be

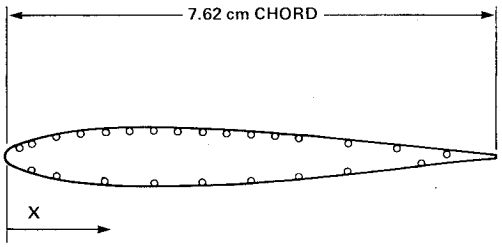

ORIFICE LOCATIONS

UPPER SURFACE		LOWER SURFACE	
X/C, %	X, cm	X/C, %	X, cm
2.5	0.191	5.0	0.381
5.0	0.381	10.0	0.762
10.0	0.762	20.0	1.524
15.0	1.143	30.0	2.286
20.0	1.524	40.0	3.046
25.0	1.905	50.0	3.810
30.0	2.286	60.0	4.572
35.0	2.667	70.0	5.334
40.0	3.046	85.0	6.477
45.0	3.425		
50.0	3.810		
55.0	4.191		
60.0	4.572		
70.0	5.334		
80.0	6.096		
90.0	6.850		

Fig. 5 NACA 0012 airfoil section with static pressure orifices.

measured. An alternative nonintrusive technique is volumetric measurements of flow through ventilated walls. It was concluded from studies carried out at Calspan[12] that the normal components of the disturbance velocity in an inviscid flow were substantially larger than indicated by the measurements made by flow meters at the wall. Apparently there is a complicated amplification in the normal velocity through the boundary layer; because the amplification depends in part on the upstream history of the boundary layer, it is not feasible to calibrate it.

Another nonintrusive technique, laser velocimetry, was considered and found to be well suited to the adaptive-wall application. Laser velocimetry was appropriate for several reasons. Besides being nonintrusive, a laser velocimeter is capable of accurately measuring vertical velocities that are small compared to the streamwise component. This was important because the maximum flow angles at level 1 were typically 6 deg or less, and flow angles at level 2, farther from the model, were even smaller. In addition, a two-dimensional traversing system allowed the laser measurement point to be positioned accurately and automatically. The design of the tunnel was also appropriate for laser velocimetry. Since both side walls of the test section were transparent, it was possible to operate the velocimeter in forward scatter, rather than back scatter. This was essential in order to achieve acceptable data rates at transonic speeds. In addition, naturally occurring dust particles were sufficient to produce acceptable data rates, thus eliminating the need to artificially seed the flow.

The laser velocimeter, illustrated schematically in Fig. 6, is similar to the laser velocimeters designed for use in the 8 × 8-in. supersonic and 2 × 2-ft transonic wind tunnels at NASA-Ames Research Center.[16] It is a one-velocity component, fringe-mode instrument. The light source was a 4-W argon-ion laser operating at a wavelength of 5145 Å. The diameter of the measurement volume was about 300 μm. Data rates were typically between 500 and 1000 signals per second.

Vertical velocities were measured directly by aligning the interference fringes, formed where the laser beams intersected, with the streamwise axis of the test section. Direct measurement was possible because a Bragg cell produced a 40

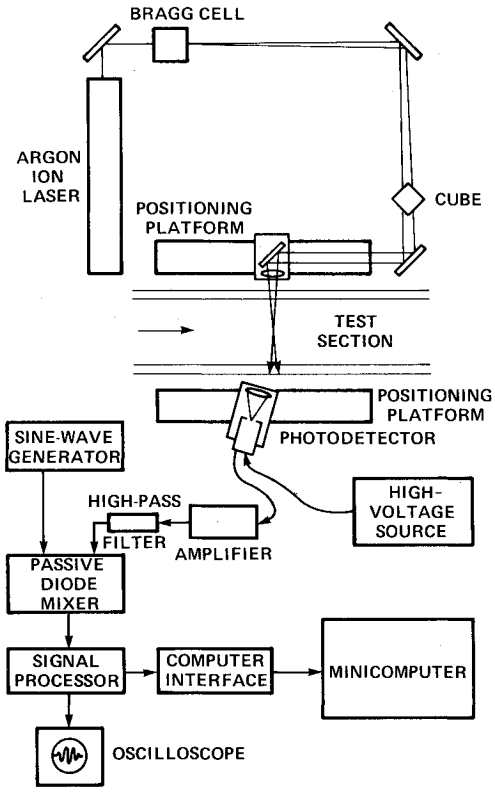

Fig. 6 Schematic of the laser velocimeter.

MHz frequency difference between the two laser beams, that caused the interference fringes to rapidly sweep across the measurement volume. Had the fringes been stationary (no Bragg cell) the light-scattering particles, whose flightpaths were nearly parallel to the fringes, would have passed through the measurement volume without crossing enough fringes (a minimum of eight was required) to produce a usable signal.

The output from the laser velocimeter signal processor was a 10-bit binary number corresponding to the time required for a particle to cross eight interference fringes in the measurement volume. Signals from particles that crossed fewer than eight fringes were not transmitted to the minicomputer.

The minicomputer accepted and stored 1000 signals from the Laser Doppler Velocimeter (LDV) signal processor at each measurement location. After acquiring the last signal, the minicomputer converted each signal to a velocity and produced an on-line graphical display of the velocity histogram. The mean velocity was computed from the histogram after elimination of all velocities that occurred less often than one-third the number of times the most frequently measured velocity occurred. This procedure eliminated biasing due to spurious signals. In general, between 80 and 90% of the data points were included in the mean velocity calculation.

The transmitting and collecting lenses were carried on platforms that were positioned along horizontal and vertical slides by lead screws driven by precision stepping motors. Control boxes commanded the motors to turn through a predetermined number of steps each time a relay was closed. One control box governed the horizontal motion of both the transmitting and collecting platforms, and a second box controlled vertical motion. The control box relays were closed and opened by a minicomputer in a sequence that positioned the laser beams at each measurement location.

V. Computer-Experiment Integration

The Eclipse minicomputer was a crucial element in the adaptive-wall system. It was used to control data acquisition

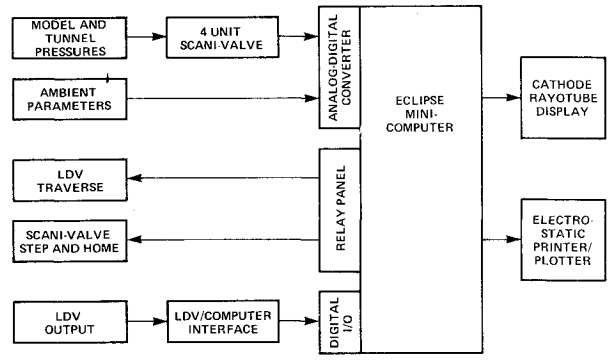

Fig. 7 Schematic of the computer interface.

for both the pressure and laser instrumentation, to provide real-time data reduction, to compute the interference-free velocity distribution at the control levels, and to compute the plenum pressure changes required to eliminate wall interference. The computer automatically controlled the sequence of events in each iteration, with the exception that the plenum pressure control valves were manually adjusted according to the computer's instructions.

The outputs from the Scanivalves, the outputs corresponding to ambient pressure and temperature, calibration pressure, and Mach number indicator are integrated with the analog-to-digital converter of the Eclipse minicomputer, as shown in Fig. 7. Each parameter is sampled 200 times with a period of 5 μs. The average value of the 200 samples is taken as the mean value for further processing.

The step and home relays of the Scanivalve are operated according to a predetermined program via the Eclipse relay closure system. The velocimeter traversing system was also interfaced to the computer-controlled relay board. Programmed switching of the relays automatically positioned the laser beams, as discussed in Sec. IV B.

The 16-bit digital output of the LV signal processor was interfaced to the Eclipse computer digital input-output system (DIOS). Ten of these bits represented a number that was a measure of each signal period (see Sec. IV B). Four bits represented an exponent that could be set to adjust the range of signal periods that could be measured. One bit was an interrupt, that indicated when a signal had been validated by the signal processor. When the data are validated they are locked until the 16 bits of data are read by the computer and stored in the memory. Then the computer signals that it is ready to accept the next data point. This process is continued until the required number of points is acquired.

VI. Wind-Tunnel Calibration

The adaptive-wall wind tunnel was calibrated in two phases: the first consisted of evaluating the Mach number distribution in the test section in the conventional manner; the second consisted of measuring influence coefficients for the individual plenums.

A. Conventional Calibration

The axial and vertical Mach number distributions in the test section were obtained from sidewall pressure measurements at the locations shown in Fig. 4. Static pressures were also measured in the upper and lower plenum compartments. Test section Mach number calibration was initially performed with the tunnel empty and with no air injection or removal from the plenum compartments. The Mach number distribution was also measured, with varying amounts of air added or removed through each compartment, during the influence-coefficient calibration (Sec. VI B).

Figure 8 illustrates typical Mach number and plenum pressure distributions with all plenum pressure control valves closed. At Mach numbers below 0.7, the standard deviation

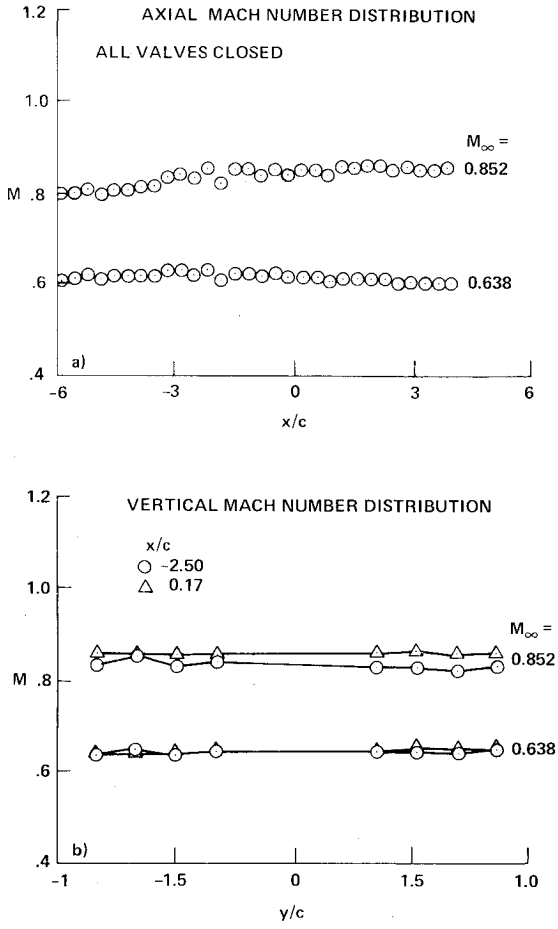

Fig. 8 Mach number and plenums pressure distribution.

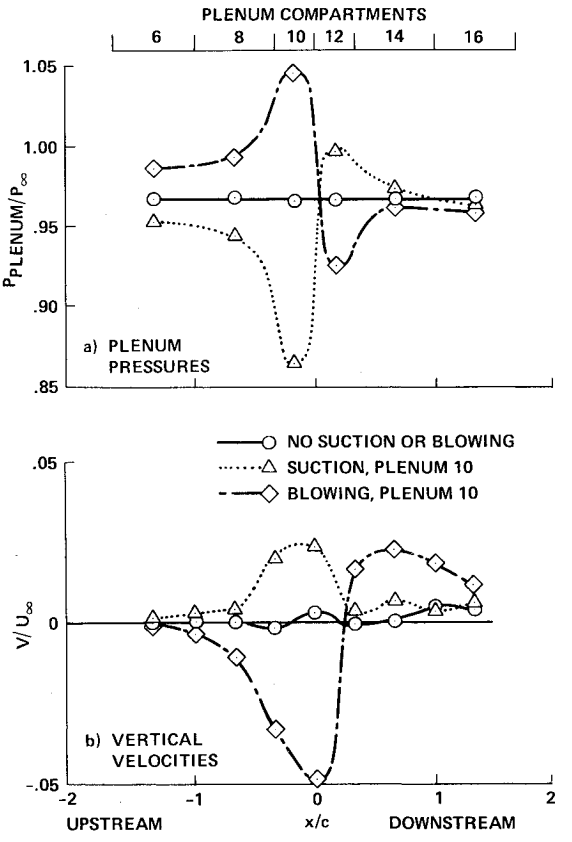

Fig. 9 Vertical velocity field.

of the axial Mach number distribution was about 0.006. At higher Mach numbers, however, there was a slight gradient. Figure 8b illustrates the Mach number distribution along vertical lines at two axial locations in the test section. The axial Mach number gradient is evident for $M=0.852$. The gradients at higher Mach numbers could easily be eliminated by appropriate plenum control.

B. Influence Coefficients

Wall interference was assessed by comparing the measured vertical velocity (v_{m2}) with the computed unconfined vertical velocity (v_{c2}) at a number of control points at level 2. The control problem was to simultaneously produce the required velocity changes at all control points by changing the pressures in the plenum compartments above and below the test section.

During the test-section calibration, the pressure in each plenum was changed progressively by opening the plenum control valve, and the resulting vertical velocity was measured at each control point at level 2; the procedure was repeated for each plenum compartment. This calibration was performed with the tunnel empty and at Mach 0.64. Initially, pressures in upper and lower compartments were adjusted symmetrically, and velocity changes were measured only at upper level 2, because the first test was of a symmetrical airfoil at zero angle of attack. Subsequent calibration prior to the lifting airfoil test revealed that pressure changes in upper compartments had no measurable effect on the vertical velocity at lower level 2 and vice versa. Therefore, it was possible to uncouple control of the upper and lower halves of the test section.

Removal or injection of air through any one of the plenum compartments altered the velocity field in the test section and also induced pressure changes in other plenum compartments. Figure 9 illustrates the vertical velocity distributions along upper level 2 for the cases of maximum symmetrical suction and blowing through plenum compartments 9 (below the test section) and 10 (above the test section). Also illustrated are the pressures measured in the upper plenum compartments. Since the influence of lower compartments at upper level 2 was negligible, these data are approximately equal to the effect of suction and blowing through compartment 10 only.

Removal or addition of mass through one plenum compartment (the "active" compartment) produced pressure changes in other compartments both upstream and downstream of the active compartment (Fig. 9a). Velocity changes were greatest immediately below the active compartment (Fig. 9b). Measurable velocity changes were produced just upstream of the active compartment for both suction and blowing; however, in the case of suction, velocity changes decreased rapidly downstream of the active compartment. Maximum blowing produced a substantial velocity disturbance at level 2 downstream of the active compartment. This disturbance, characterized by highly turbulent flow, did not extend to level 1 or to the model.

Figure 10a illustrates the influence of symmetric pressure changes in compartments 11 and 12 on the vertical velocities at several points at the upper level 2. Figure 10b is a similar plot showing the influence at a single point at upper level 2 of pressure changes in different plenum compartments. For small pressure changes, the relationships between pressure and velocity changes are quite linear. Therefore, an influence coefficient, defined as the slope $\Delta V_i/\Delta P_j$, was used to describe the influence of pressure changes in compartment j on the vertical velocity at control point i (level 2).

The combined influence on the velocity at a point of pressure changes in more than one compartment was assumed to be equivalent to the sum of the velocity changes produced at that point by the same pressure changes in each compartment taken separately. By assuming linear superposition it was possible to relate velocity changes at the level 2 control

points to the pressure changes in the plenum compartments:

$$\begin{bmatrix} \Delta V_1 \\ \Delta V_i \\ \Delta V_N \end{bmatrix} = \begin{bmatrix} \frac{\Delta V_1}{\Delta P_1} \cdots \frac{\Delta V_1}{\Delta P_M} \\ \frac{\Delta V_i}{\Delta P_j} \\ \frac{\Delta V_N}{\Delta P_1} \quad \frac{\Delta V_N}{\Delta P_M} \end{bmatrix} \begin{bmatrix} \Delta P_1 \\ \Delta P_j \\ \Delta P_M \end{bmatrix}$$

or $\Delta V_i = C_{ij}\Delta P_j$. In the preceding equation, the unknowns are the pressure changes ΔP_j necessary to produce the required velocity changes ΔV_i. If the influence coefficient matrix is square—that is, there are as many control points as plenum compartments—then the compartment pressures may be computed after inverting the influence coefficient matrix and multiplying by the required velocity changes:

$$\Delta P_j = C_{ij}^{-1}\Delta V_i$$

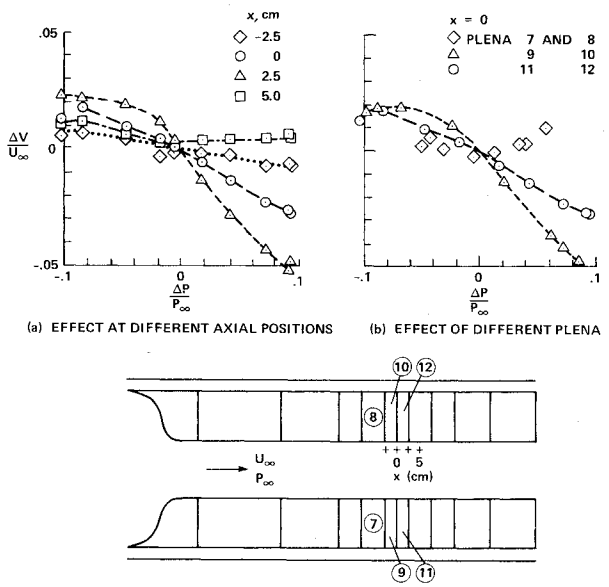

Fig. 10 Typical influence coefficients.

VII. Implementation of Adaptive-Wall Wind-Tunnel Scheme

Experiments were conducted in the adaptive-wall wind tunnel on the NACA 0012 airfoil at angles of attack of 0 and +2 deg and at different Mach numbers, with and without a boundary-layer trip. Here, a typical case—a supercritical Mach number of $M = 0.788$ at zero incidence with the boundary-layer trip—is discussed to illustrate the implementation of the adaptive-wall scheme.

Initially the downstream throat position was adjusted to obtain the required approach Mach number, and all the plenums were set to any suitable initial position. The data acquisition sequence begins with laser velocimeter measurements at the control points at levels 1 ($y/c = 0.40$) and 2 ($y/c = 0.67$). Level 1 velocities were measured at 15 control points; the points were 2.54 cm apart, beginning 2 chord lengths upstream of the model leading edge. At level 2, the velocity was measured at 9 control points; the points were 2.54 cm apart, beginning 1 chord length upstream of the model leading edge and ending ⅔ chord lengths downstream of the trailing edge. After the data were acquired at each point, on-line computations of the mean velocity and other flow parameters were displayed on the CRT. After all laser velocimeter measurements were completed, the velocimeter returned to its starting point and the computer presented a graphical display on the CRT of the velocity distributions at levels 1 and 2. Next, the Scanivalve readings—including model pressures, axial and vertical static pressure distributions, and plenum compartment pressures and other ambient conditions—were acquired and all the data were

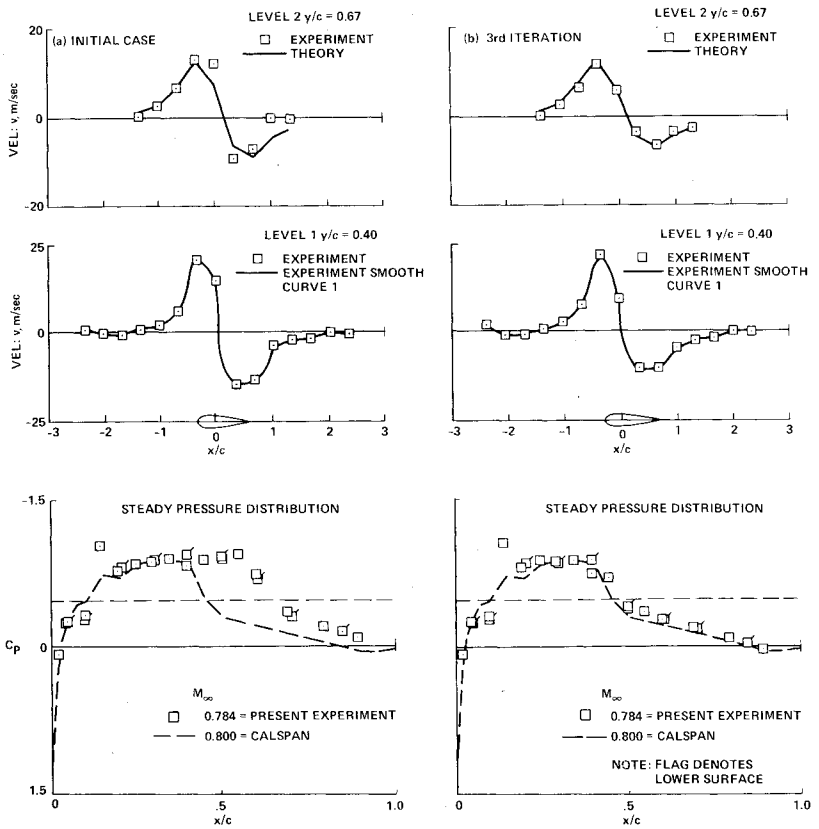

Fig. 11 Vertical velocity and model pressure distribution.

displayed on the CRT to allow observation of improvements after each iteration. During routine testing these data need be acquired only at the end of the final iteration.

The entire data acquisition sequence for a symmetric flowfield takes about 10 min. Of this time, about 6 min are spent acquiring and reducing laser data, about 2.5 min are spent while the velocimeter traverses between measurement points, and about 1.5 min are spent acquiring and reducing the Scanivalve data. In an optimized system, the laser velocimeter data acquisition and traversing times would be substantially reduced.

After the velocity and pressure data have been acquired and reduced, the wall interference is displayed graphically and the plenum pressure changes required to eliminate this interference are computed, using the influence-coefficient matrix. In general, only six control points were selected for correction because only six top and six bottom plenum compartments were capable of producing measurable velocity changes at the selected control points. The plenum compartments farthest removed from the model had no measurable influence on the flowfield near the model. Plenum compartment pressures were adjusted by manually turning the appropriate valves of the auxiliary air system and noting the resulting pressure changes observed on a manometer board. For zero incidence of the symmetric model, upper and lower plenum pressures were adjusted symmetrically. For the case of nonzero incidence, the upper and lower plenums were adjusted assuming the upper half had no appreciable effect on the lower half, and vice versa.

After adjusting the appropriate plenums pressures, the experiment was repeated. These iterations were carried out until the required accuracy was obtained or until no further improvements were observed. This goal is usually achieved in about three iterations.

The measured and calculated vertical velocity components at levels 1 and 2 for a typical case at $M=0.788$ and at zero incidence are presented in Fig. 11. The measured pressure distribution over the airfoil is compared with the Calspan results.[17] The Calspan data, obtained on a 15.2 cm (6 in.) chord airfoil tested in their 2.4 m (8 ft) wind tunnel, are considered to be interference free. The results of the initial case or zeroth iteration are presented in Fig. 11a and the results of the third iteration are presented in Fig. 11b. Initially, the deviations in the vertical velocity components at level 2 are considerable, indicating the results are not interference free. This can be readily observed from the pressure distribution. The shock-wave position is off by more than 15% of chord. The third iteration measurements of vertical velocity components compared well with the calculated results. The corresponding C_p distribution and shock-wave position matched reasonably well with the Calspan results, indicating convergence of the results. The upper surface boundary-layer trip in the present experiment is responsible for the anomalous pressure measurement 0.14 chord aft of the airfoil leading edge.

VIII. Conclusions and Suggestions

Computer experiment integration with on-line data acquisition was successfully applied in the adaptive wind-tunnel experiments using nonintrusive instrumentation. The influence coefficient matrix method was successfully applied to obtain convergence to interference-free flow, thus showing the practicality of the adaptive-wall wind tunnel.

Some further research needs to be done to make the adaptive-wall wind tunnel suitable for routine testing. The time to acquire LDV data should be decreased, and the possibility of using one-step algorithms should be investigated. On-line theoretical computations should be expanded to the case of fully transonic flows, and the possibility of investigating three-dimensional flow should be explored with the techniques used in this paper.

References

[1] Kemp, W.B. Jr., "Toward the Correctable-Interference Transonic Wind Tunnel," *Proceedings of the AIAA 9th Aerodynamic Testing Conference,* June 1978, pp. 31-38.

[2] Kemp, W.B. Jr., "Transonic Assessment of Two-Dimensional Wind Tunnel Wall Interference Using Measured Wall Pressures," NASA Conference on Advanced Technology Airfoil Research, Langley, Va., March 1978.

[3] Stahara, S.S. and Spreiter, J.R., "A Transonic Wind Tunnel Interference Assessment - Axisymmetric Flows," AIAA Paper 79-0203, Jan. 1979.

[4] Murman, E.M., "A Correction Method for Transonic Wind Tunnel Wall Interference," AIAA Paper 79-1533, July 1979.

[5] Hilton, W.F., *High-Speed Aerodynamics,* Longman, Green and Co., New York, 1951, pp. 389-391.

[6] Ferri, A. and Baronti, P., "A Method for Transonic Wind Tunnel Corrections," *AIAA Journal,* Vol. 11, Jan. 1973, pp. 63-66.

[7] Sears, W.R., "Self Correcting Wind Tunnels," *Aeronautical Journal,* Vol. 78, Feb.-March 1974, pp. 80-89.

[8] Sears, W.R., "A Note on Adaptive Wall Wind Tunnels," *Zeitschrift fuer Angewandte Mathematik und Physik,* Vol. 28, 1977, pp. 915-927.

[9] Lo, C.F. and Kraft, E.M., "Convergence of the Adaptive-Wall Wind Tunnel," *AIAA Journal,* Vol. 16, Jan. 1978, pp. 67-72.

[10] Sears, W. R., "Adaptive Wind Tunnels with Imperfect Control," *Journal of Aircraft,* Vol. 16, May 1979, pp. 344-348.

[11] Erickson, J.E. Jr. and Nenni, J.P., "A Numerical Demonstration of the Establishment of Unconfined-Close Conditions in a Self-Corrective Wind Tunnel," Calspan Rept. RK-5070-A-1, Nov. 1973.

[12] Vidal, R.J., Erickson, J.C. Jr., and Catlin, P.A., "Experiments with a Self-Correcting Wind Tunnel," *AGARD Conference Proceedings No. 174,* March 1976.

[13] Goodyer, J.J., "A Low Speed Self Streamlining Wind Tunnel," *AGARD Conference Proceedings No. 174,* March 1976.

[14] Ganzer, U., "Wind Tunnels with Adapted Walls for Reducing Wall Interference," *Zeitschrift fuer Flugwiss. Weltraumforsch.,* Vol. 3, March-April 1979, pp. 129-133.

[15] Kraft, E.M. and Parker, R.L. Jr., "Experiments for the Reduction of Wind Tunnel Interference by Adaptive-Wall Technology," AEDC-TR-79-51, Oct. 1979.

[16] Johnson, D.A., Bachalo, W.D., and Moddaress, D., "Laser Velocimetry Applied to Transonic and Supersonic Aerodynamics," *AGARD Conference Proceedings No. 193,* May 1976.

[17] Vidal, R.K., Catlin, P.A., and Chudyk, D.W., "Two-Dimensional Subsonic Experiments with a NACA 0012 Airfoil," Calspan Rept. RK-5070-A-3, Dec. 1973.